Available online at www.sciencedirect.com

SciVerse ScienceDirect

journal homepage: www.elsevier.com/locate/issn/15375110

Research Paper

A methodology for model-based greenhouse design: Part 2, description and validation of a tomato yield model

B.H.E. Vanthoor [a,b], P.H.B. de Visser [a], C. Stanghellini [a], E.J. van Henten [a,b,*]

[a] Wageningen UR Greenhouse Horticulture, P.O. Box 644, NL-6700 AP Wageningen, The Netherlands
[b] Farm Technology Group, Wageningen University, P.O. Box 17, NL-6700 AA Wageningen, The Netherlands

ARTICLE INFO

Article history:
Received 6 July 2010
Received in revised form
17 July 2011
Accepted 17 August 2011
Published online 5 October 2011

With the aim of developing a model-based method to design greenhouses for a broad range of climatic and economic conditions, a tomato yield model that describes the effects of greenhouse climate on yield was described and validated. A literature survey of temperature effects on tomato yield was performed and the main temperature effects were implemented in the model. Subsequently, the yield model was validated for four temperature regimes. Results demonstrated that the tomato yield was simulated accurately for both near-optimal and non-optimal temperature conditions in the Netherlands and southern Spain, respectively, with varying light and CO_2-concentrations. In addition, the adverse effects of extremely low as well as high mean temperatures on yield and timing of first fruit harvest were simulated with fair accuracy. The simulated yield response to extreme diurnal temperature oscillations were in agreement with literature values. Given these results, the model is considered to be sufficiently accurate to be used for developing a model-based greenhouse design method. Therefore, the presented model will be integrated in a model-based design method with the aim to design the best greenhouse for local climate and economic conditions.

1. Introduction

Greenhouse design is a multi-factorial optimisation problem that relies on a quantitative trade-off between the economic return of the crop and the costs associated with construction, maintenance and operation of the greenhouse facility (Van Henten et al., 2006). As suggested by Baille (1999), a systematic approach that integrates physical, biological and economic models is the most promising way for strategic decision making on greenhouse configuration for world-wide climate conditions. To solve this optimisation problem, we developed a model-based greenhouse design method. This method is able to design greenhouses for a broad range of climatic and economic conditions. The key components of the method are a greenhouse climate model, a tomato yield model, an economic model and an optimisation algorithm as presented in Fig. 1. As a first step, this method focuses on the optimisation of the selection of alternatives to fulfil the following eight design elements: the type of greenhouse structure, the cover type, the outdoor shade screen, the whitewash, the thermal screen, the heating system, the cooling system and the CO_2 enrichment

* *Corresponding author*. Wageningen UR Greenhouse Horticulture, P.O. Box 644, NL-6700 AP Wageningen, The Netherlands. Tel.: +31 317 483328; fax: +31 317 423110.
E-mail addresses: bvanthoor@hortimax.com (B.H.E. Vanthoor), eldert.vanhenten@wur.nl (E.J. van Henten).
1537-5110/$ – see front matter © 2011 Published by Elsevier Ltd on behalf of IAgrE.
doi:10.1016/j.biosystemseng.2011.08.005

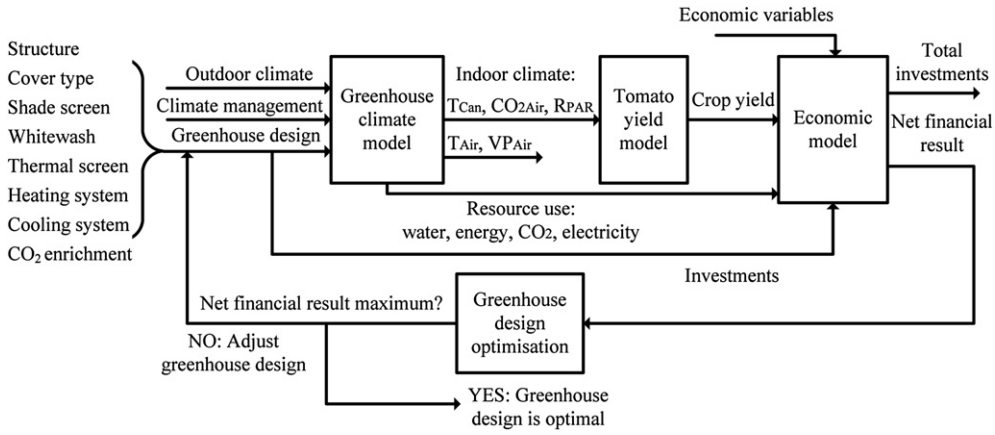

Fig. 1 – An overview of the model-based greenhouse design method. The method focuses on the optimisation of the following eight design elements: the type of greenhouse structure, the cover type, the outdoor shade screen, the whitewash, the thermal screen, the heating system, the cooling system and the CO_2 enrichment system. The key components of the method are a greenhouse climate model (Vanthoor et al., 2011), a tomato yield model, an economic model and an optimisation algorithm. The tomato yield model is described in this study.

system. This paper contains a description and validation of the tomato yield model.

Since greenhouse design affects crop yield through its effect on indoor climate, a model is presented that describes tomato (*Lycopersicon esculentum*) yield as a function of indoor climate. For use in design and optimisation studies, the model should fulfil three requirements:

1. To describe the effects of the indoor temperature, light, and CO_2-concentration on tomato yield.
2. To describe adverse effects of extremely low as well as high temperatures on tomato yield since the solution of a greenhouse design optimisation problem is expected to allow these extreme temperatures in order to save energy and investment.
3. The model should consist of a set of first order differential equations since it will be combined with a greenhouse climate model consisting of a set of differential equations and to allow the use of ordinary differential equation solvers. In addition, the right-hand sides must be continuously differentiable to speed up the simulation and to ensure that gradient-based dynamic optimisation algorithms can be applied to the model.

In the literature, several models can be found that describe the influence of light, temperature and CO_2-concentration on tomato yield. However, these models are mostly valid for relatively small temperature ranges (Ooteghem, 2007; Seginer, Gary, & Tchamitchian, 1994; Tap, 2000) and are not fully differentiable e.g. TOMGRO (Dayan et al., 1993; Jones, Dayan, Allen, Van Keulen, & Challa, 1991), TOMSIM (Heuvelink, 1996), and the tomato yield model of De Koning (1994).

In conclusion, the literature review revealed that a tomato yield model satisfying the predefined requirements is still missing and therefore the aim of this work was to describe and validate such a tomato yield model. Due to the aim of the model (to use it in a model-based greenhouse design method), the primary focus of this paper is to describe the extreme temperature effects on tomato dry matter yield.

The outline of this paper is as follows. First, since the model should deal with extreme temperatures, a literature survey of temperature effects on tomato yield is presented. Secondly, the model implementation of these main temperature effects is described. Subsequently, the simulated tomato yield is validated with the measured tomato yield for the following three temperature regimes: 1) mild temperatures with varying light and CO_2 conditions in two Dutch greenhouses; 2) extreme temperature conditions with varying light and CO_2 conditions in a low-tech greenhouse and a high-tech greenhouse in southeast Spain and 3) four constant temperature trajectories varying from sub-optimal to supra-optimal temperatures conducted in growth chambers. In addition, the effect of extreme temperature regimes is evaluated and compared with data found in the literature.

2. Temperature effects on tomato yield

Temperature influences different aspects of tomato growth (e.g., production rate and partitioning, dry matter content) and development (e.g., leaf and truss appearance, fruit growth period, abortion and fruit quality) (De Koning, 1994; Van Der Ploeg & Heuvelink, 2005). Photosynthesis, which depends on light, CO_2 and temperature, produces carbohydrates needed for crop growth. These carbohydrates are distributed to fruits, leaves, stems and roots and are converted to dry matter (such as sugars, amino acids and organic acids). The sugars fulfil the energy requirement for maintenance processes and growth processes. Finally, fruit set, fruit growth and abortion rates determine how much of the potentially available carbohydrates are allocated to the fruits.

Table 1 – A summary of effects of low and high temperatures on crop growth processes and crop yield levels based on a literature review.

Process	Period	Temperature	Results	Author
Photosynthesis	14 days	10 °C at photoperiod	2–5% of initial photosynthesis	Yakir et al., 1986
Photosynthesis	3 days after 14 days treatment	10 °C at photoperiod	Recovering to 50% of initial photosynthesis	Yakir et al., 1986
PSII electron transport	3 h	43 °C	Significant decrease compared to 25 °C	Heckathorn et al., 1998
Photosynthesis	2 h	40 °C	Reduced to 30%	Camejo et al., 2005
Fruit development time	Total production period*	14 °C mean	94.8 days 205% of 22 °C mean	Adams et al., 2001
Fruit development time	Total production period*	26 °C mean	41.5 days 89.6% of 22 °C mean	Adams et al., 2001
Fruit development time	Total production period	Between 17 °C and 26 °C	Fruit development rate is linearly related to temperature	De Koning, 1994
Fruit size	Total production period*	14 °C mean	18.3 g 36% of 22 °C mean	Adams et al., 2001
Fruit size	Total production period*	26 °C mean	23.9 g 47% compared to 22 °C mean	Adams et al., 2001
Abortion	3 weeks	6 °C constant	irreversible damage	Brüggemann et al., 1992
Fruit set/abortion	Total production period*	14 °C mean	59% compared to 22 °C mean	Adams et al., 2001
Fruit set/abortion	Total production period	28/22 °C	>75% (for all cultivars)	Sato et al., 2000
Fruit set/abortion	Total production period	32/26 °C	0% (for 4 out 5 cultivars)	Sato et al., 2000
Fruit set/abortion	Total production period	25 °C mean	48%	Peet et al., 1997
Fruit set/abortion	Total production period	29 °C mean	11%	Peet et al., 1997
Fruit set/abortion	Total production period*	26 °C mean	40% compared to 22 °C mean	Adams et al., 2001
Crop production	Continuous	12 °C mean	0%	Criddle et al., 1997
Crop production	During night	8.2 °C mean	46% compared to 11.5 °C mean	Baytorun et al., 1999
Crop production	During night	13.2 °C mean	108% compared to 15.2 °C mean	Martínez Mirón, 2008
Crop production	During night	12 °C	1571 g plant^{-1} 76% of 18 °C night	Khayat et al., 1985
Crop production	Total production period*	14 °C mean	2.2 kg FW plant^{-1} 21% of 22 °C mean	Adams et al., 2001
Crop production	Total production period*	18 °C mean	7.7 kg FW plant^{-1} 75% of 22 °C mean	Adams et al., 2001
Crop production	Total production period*	26 °C mean	1.9 kg FW plant^{-1} 18% of 22 °C mean	Adams et al., 2001
Crop production	Total production period	29 °C mean	117.32 g plant^{-1} 17% compared to 25 °C mean	Peet et al., 1997
Crop production	Day time	35 °C	46.1% compared to 25 °C	Zhang et al., 2008
Crop growth	Daily	DIF = −6 °C (day 18 °C and night 24 °C)	Reduced plant growth and development	Heuvelink, 1989
Crop growth	Daily	DIF = 10 °C (day 26 °C and night 16 °C)	Similar growth and development to DIF = 2 °C (day 22 °C and night 20 °C)	Heuvelink, 1989
Crop production	Production rate period	DIF = 14 °C	Higher production compared to 5 °C DIF	Gent & Ma, 1998
Crop production	Production rate period	DIF = 18 °C	Similar production to a DIF is 6 °C	Mavrogianopoulos, Kyritis, 1989

The * indicates that the treatment started 21 days after sowing.

In this section, a literature study of the effects of sub-optimal, supra-optimal and (large) differences between day and night temperature on growth, development and ultimately on tomato yield is presented. As it is not exhaustive, this survey is only expected to capture the main trends. Although the impact of temperature depends on the associated solar radiation, CO_2-concentration and humidity levels, the focus of this survey was to capture the main temperature trends based on temperature experiments with naturally varying levels of the other climatic factors. The impact of supra-optimal temperature on growth implicitly comprises the negative effect of high vapour pressure deficit (VPD) on growth. Specifically, a high VPD is strongly correlated to a high temperature so that uncoupling these factors seemed superfluous. Results of this survey are summarised in Table 1.

2.1. *The effect of sub-optimal temperatures on fruit fresh weight yield*

Chilling temperatures may affect negatively photosynthesis, respiration, membrane integrity, water relations, the hormone balance of the plants and fruit set (Adams, Cockshull, & Cave, 2001; Brüggemann, van der Kooij, & van Hasselt, 1992; Van Der Ploeg & Heuvelink, 2005; Yakir, Rudich, & Bravdo, 1986). Additionally, the fruit growth period increases with decreasing temperatures (De Koning, 1994). These unfavourable processes decrease the total fruit fresh weight.

Below a mean temperature of 12 °C, Criddle, Smith, and Hansen (1997) observed no significant growth and tomato yield. Khayat, Ravad, and Zieslin (1985) found that, with similar solar radiation levels, the cultivar Moneymaker grown at a night temperature of 12 °C yielded only 76% of the yield observed at 18 °C. However, the same treatment for the cultivar Cherry did not affect growth. These results indicate that the impact of low temperature on crop yield is cultivar-dependent.

According to Baytorun, Topçu, Abak, and Daşgan (1999), yield levels of plants exposed for 3 months to a minimum mean night temperature of 8.2 °C decreased to 46% compared to levels observed at a minimum mean night temperature of 11.5 °C with similar solar radiation levels. Furthermore, Adams et al. (2001) observed at a mean temperature of 14 °C, a yield decrease to 21% of the crop yield observed at 22 °C with other climatic factors remaining similar. Additionally, Adams et al. (2001) found that fruits grown at a mean temperature of 14 °C were parthenocarpic, small, hard and without economical value.

In contrast to the above-mentioned results, Martínez Mirón (2008) observed under relatively low light conditions (mean global radiation sum of 7.6 MJ m^{-2} day^{-1}) at a mean minimum night temperature of 13.2 °C, a yield increase to 108% of the yield observed at 15.2 °C. At higher light levels (9.4 MJ m^{-2} day^{-1}) no positive effect of a low mean night temperature on crop yield was observed. These results indicate that under low light conditions, low rather than high mean night temperature may favour crop growth. However, the general trend observed in the literature was that yield decreased with decreasing night temperatures.

2.2. *The effect of supra-optimal temperatures on fruit fresh weight yield*

At supra-optimal levels, the instantaneous temperature decreased photosynthesis and the mean temperature caused a lower fruit set, shorter fruit growth period and smaller fruits (Adams et al., 2001; Camejo et al., 2005; De Koning, 1994; Heckathorn, Downs, Sharkey, & Coleman, 1998; Peet, Willits, & Gardner, 1997; Sato, Peet, & Thomas, 2000). These unfavourable processes decreased the total fruit fresh weight. Adams et al. (2001) reported that a mean temperature of 26 °C reduced crop yield to 18% of that at 22 °C and Peet et al. (1997) observed that a mean temperature of 29 °C reduced crop yield to 17% of that at 25 °C with similar radiation levels. Zhang, Li, and Xu (2008) observed at a day temperature of 35 °C a crop yield decrease to 46.1% compared to a day temperature of 25 °C.

2.3. *The effects of both short term and long term temperature differences*

The difference between day and night temperature (DIF) also affects crop growth processes. For young tomato plants, Heuvelink (1989) found that, for similar mean temperatures, a lower day than night temperature (DIF = −6 °C) reduced plant growth and development (number of leaves and number of trusses) with respect to a treatment with a DIF of 2 °C with similar radiation levels. Yet, for a large positive DIF of 10 °C, Heuvelink (1989) observed a growth rate and development rate similar to a DIF of 2 °C. Gent and Ma (1998) observed that crops grown at a DIF of 14 °C yielded more fruit fresh weight than those grown under 5 °C DIF with similar radiation levels whereas Mavrogianopoulos and Kyritis (1989) observed similar crop yield levels in warm climates at a DIF of 6 °C and 18 °C. The negative effects of a large positive DIF on crop yield should be seen as a result of non-optimal temperature levels (i.e. caused by sub-optimal night temperature and/or supra-optimal day temperature) rather than day–night differences per se.

2.4. *Temperature dependent growth rate responses and model implementation*

Summarising, the literature survey indicated that a) both instantaneous and mean temperatures affect crop yield, b) both sub-and supra-optimal temperatures affect several growth processes, resulting in lower yield, c) it is difficult to identify one single growth process causing crop stress because growth processes influence each other, d) stress sensitivity is cultivar-dependent and e) a negative DIF and a large positive DIF negatively affect crop yield due to sub-or supra-optimal temperatures.

Since the crop yield model will be integrated in a model-based design method, detailed modelling of the effects of non-optimal temperatures on individual crop growth processes was beyond the scope of this research. In contrast, a model was developed that captures the temperature dependency of various processes by means of two lumped temperature-dependent growth inhibition functions. These inhibition functions capture the instantaneous and the mean temperature effects on overall tomato yield by multiplying the potential tomato growth rate by these inhibition functions ($0 \leq$ inhibition function ≤ 1). These growth inhibition functions will implicitly take into account also the impact of large VPD on growth processes because a large VPD mainly occurs at a supra-optimal temperature. Abortion processes were already captured by the two lumped temperature-dependent growth inhibition functions and were therefore not modelled explicitly.

3. Model overview and states

3.1. *Notational conventions*

To describe the states and the flows of the tomato yield model the notational conventions of De Zwart (1996) are used. The states of the model are denoted by names with capital letters followed by one subscript (Table 2 and Table 3). The flows are denoted by a capital letter followed by two subscripts. The first subscript represents the source of the flow and the second subscript represents the destination of the flow. For example, MC_{AirBuf} denotes the carbon flow from air to the carbon buffer. The surface unit is m^2 of greenhouse floor, unless specified otherwise. For clarity, all carbohydrates are expressed in mg $\{CH_2O\}$ m^{-2}. When leaving the carbohydrate buffer, these carbohydrates transform from non-structural carbohydrates to dry matter since growth respiration is removed from the carbohydrate buffer prior to partitioning. The model parameters are listed in Table 4.

Table 2 – State, semi-state and flows used in the model.

	Name	Unit
States		
C	Carbohydrate amount	mg {CH_2O} m^{-2}
DM	Dry matter	mg {DM} m^{-2}
N	Number	fruits m^{-2}
T	Temperature	°C
TS	Temperature sum	°C d
Semi-state		
LAI	Leaf Area Index	m^2 {leaf} m^{-2}
Flow		
MC	Carbohydrate mass flow	mg {CH_2O} m^{-2} s^{-1}
MN	Number flow	fruits m^{-2} s^{-1}

3.2. *Model overview*

The model structure, with a common carbohydrate buffer and carbohydrate distribution to plant organs as presented in Fig. 2, was essentially based on earlier crop yield models (Dayan et al., 1993; Heuvelink, 1996; Marcelis, Heuvelink, & Goudriaan, 1998; Linker, Seginer, & Buwalda, 2004; Seginer et al., 1994) and extended with the two lumped temperature-dependent growth inhibition functions. A temperature sum representing the development stage of the crop was modelled to define the timing of first fruit set and the time at which the carbohydrate distribution to the fruits reaches its potential.

Photosynthesis MC_{AirBuf} depends mainly on the canopy temperature, the photosynthetically active radiation (PAR) absorbed by the canopy and the CO_2-concentration in the greenhouse. When relating crop growth directly to photosynthesis without using a carbohydrate buffer, the impact of night temperature on growth would be neglected. However, night temperatures play an important role in crop growth and development. To model the effects of night temperature on growth and development, the photosynthesised carbohydrates are stored in a buffer, C_{Buf}, whose outflow is affected by temperature. The buffer distributes the carbohydrates ($MC_{BufFruit}$, $MC_{BufLeaf}$, $MC_{BufStem}$) to the plant organs (C_{Fruit}, C_{Leaf}, C_{Stem}) even when no photosynthesis occurs. These carbohydrate flows are influenced by the availability of carbohydrates in the buffer, the organ growth rate coefficients, two temperature-dependent growth inhibition functions (each described as function of the instantaneous temperature, T_{Can}, and the 24 h mean temperature,T^{24}_{Can}) and the temperature sum, TS_{Can}, representing the development stage of the crop.

The plant organ C_{Stem} represents the carbohydrates which are stored in both stem and root. To take into account the time delay between fruit set and fruit harvest, the model simulates for each fruit development stage, *j*, the fruit weight $C_{Fruit\{j\}}$ and the fruit numbers $N_{Fruit\{j\}}$. A part of the carbohydrates in the organs is used for maintenance respiration ($MC_{FruitAir}$, $MC_{LeafAir}$, $MC_{StemAir}$). When the leaf area index (LAI) exceeds a maximum value, LAI^{Max}, the leaves are pruned back to this value, resulting in the mass flow $MC_{LeafHar}$. The accumulated harvested tomato dry matter is determined by integrating the carbohydrate outflow of the last fruit development stage.

The state variable equations and the carbohydrate flow to the individual plant organs with special interest for the two lumped temperature-dependent growth inhibition functions are presented in this chapter. Because of space limitations, the remaining model processes are presented in the electronic appendix (e-appendix). A brief description of these model processes is given here.

The PAR absorbed by the canopy is described by a negative exponential decay of light intensity with LAI in a homogeneous row crop as described by Ross (1975). As described in detail in the e-appendix, the canopy photosynthesis is determined by performing the following 5 steps: (I) the maximum rate of electron transport at 25 °C at canopy level is calculated as described by Evans and Farquhar (1991) by multiplying the LAI with the maximum rate of electron transport at leaf level at 25 °C ($J^{MAX}_{25,Leaf} = 210$ μmol {e^-} m^{-2} {leaf} s^{-1}, parameter value derived by Farquhar, Caemmerer, and Berry (1980)); (II) the potential rate of electron transport is calculated by multiplying the maximum rate of electron transport at 25 °C at canopy level by the temperature function as described by (Farquhar et al., 1980) with the following parameters: the activation energy ($E_j = 37 \times 10^3$ J mol^{-1}), the entropy term ($S = 710$ J mol^{-1} K^{-1}) and the deactivation energy ($H = 22 \times 10^4$ J mol^{-1}); (III) the electron transport rate is determined as a function of the potential rate of electron transport and of the PAR absorbed by the canopy (Evans & Farquhar, 1991; Farquhar, 1988) with the following parameters: the conversion factor from photons to electrons ($\alpha = 0.385$ μmol {e^-} μmol^{-1} {photons}) and the degree of curvature of the electron transport rate ($\Theta = 0.7$); (IV) the gross photosynthesis rate at canopy level is calculated based on Farquhar (1988) as a function of the electron transport rate, the CO_2-concentration in the stomata and the CO_2 compensation point; (V) the net photosynthesis rate equals the gross photosynthesis rate minus photorespiration (Farquhar & von Caemmerer, 1982) multiplied by the photosynthesis inhibition factor ($0 < h < 1$) caused by saturation of the carbohydrate buffer. The impact of rubisco on photosynthesis depends highly on the stomatal behaviour of the leaves which in turn is strongly affected by extreme temperatures. In this research it was assumed that that the two temperature-dependent growth inhibition functions implicitly described the impact of rubisco on the photosynthesis rate.

Even though VPD strongly affects stomatal conductance, photosynthesis is not sensitive to VPD (Stanghellini &

Table 3 – Subscripts and superscripts used in the model.

Subscripts	Name	Subscripts	Name
24	Mean of 24 h	*j*	Fruit development stage
Air	Air	*Leaf*	Leaves
Buf	The carbon buffer	*Start*	Start of period
Can	Canopy	*Stem*	Stem and roots
End	End of period	Superscripts	
Fruit	Fruit	*Max*	Maximum
Har	Harvest	*Min*	Minimum
Inst	Instantaneous temperature effect	*Sum*	Summation

Table 4 – List of model parameters and symbols. The determination of some model parameters is presented in the electronic appendix (e-appendix).

Parameter	Symbol and value	Unit	Reference
Conversion factor from carbohydrate to dry matter	$\eta_{C\_DM} = 1$	mg {DM} mg^{-1} {CH_2O}	Growth respiration was described and no lignification assumed
The time constant to calculate the 24 h mean temperature	$\tau = 86{,}400$	s	See the e-appendix, Appendix A
Maximum buffer capacity	$C_{Buf}^{Max} = 20 \times 10^3$	mg {CH_2O} m^{-2}	See the e-appendix, Section 4.1
Minimum amount of carbohydrates in the buffer	$C_{Buf}^{Min} = 1 \times 10^3$	mg {CH_2O} m^{-2}	See the e-appendix, Section 4.2
The gain of the process to calculate the 24 h mean temperature	$k = 1$	–	See the e-appendix, Appendix A
Potential fruit growth rate coefficient at 20 °C	$rg_{Fruit} = 0.328$	mg {CH_2O} m^{-2} s^{-1}	See the e-appendix, Appendix C. Determined based on (De Koning, 1994)
Potential leaf growth rate coefficient at 20 °C	$rg_{Leaf} = 0.095$	mg {CH_2O} m^{-2} s^{-1}	See the e-appendix, Appendix C. Determined based on Heuvelink (1996)
Potential stem growth rate coefficient	$rg_{Stem} = 0.074$	mg {CH_2O} m^{-2} s^{-1}	See the e-appendix, Appendix C. Determined based on Heuvelink (1996)
Specific leaf area index	$SLA = 2.66 \times 10^{-5}$	m^2 {leaf} mg^{-1} {CH_2O}	Assumed to be constant, based on Heuvelink (1996)
Temperature sum when fruit growth rate is at full potential	$TS_{End}^{Sum} = 1035$	°C d	Based upon Eq. (31) of the e-appendix
Base temperature for 24 h mean crop growth inhibition	$T_{Base\_24} = 12$	°C	See the e-appendix, Appendix C
First optimal temperature for 24 h mean crop growth inhibition	$T_{Opt1\_24} = 18$	°C	See the e-appendix, Appendix C
Second optimal temperature for 24 h mean crop growth inhibition	$T_{Opt2\_24} = 22$	°C	See the e-appendix, Appendix C
Maximum temperature for 24 h mean crop growth inhibition	$T_{Max\_24} = 27$	°C	See the e-appendix, Appendix C
Base temperature for instantaneous crop growth inhibition	$T_{Base\_Inst} = 6$	°C	See the e-appendix, Appendix C
First optimal temperature for instantaneous crop growth inhibition	$T_{Opt1\_Inst} = 14$	°C	See the e-appendix, Appendix C
Second optimal temperature for instantaneous crop growth inhibition	$T_{Opt2\_Inst} = 28$	°C	See the e-appendix, Appendix C
Maximum temperature for instantaneous crop growth inhibition	$T_{Max\_Inst} = 40$	°C	See the e-appendix, Appendix C

Bunce, 1993). Therefore, VPD effects on canopy photosynthesis rate were not incorporated in the model. For the purpose of model-based greenhouse design, the crop yield model will be combined with a greenhouse climate model (Vanthoor, Stanghellini, Van Henten, & De Visser, 2011) that calculates the canopy temperature using the transpiration and stomatal model of Stanghellini (1987). Consequently, the modelled thermal and hydraulic feedback systems ensure that VPD affects the temperature-dependent growth inhibition functions and crop growth through its effect on canopy temperature. The fruit flow and carbohydrate flow to fruit development stages and the daily potential growth rate per fruit for different fruit development stages are based on De Koning (1994). The growth and maintenance respiration are based on Heuvelink (1996).

3.3. *State variables of the model*

The state variables of the model are all described by differential equations. The time derivatives of the state variables are indicated by a dot above the state symbol.

The development rate of the plant, which determines the transition from the vegetative to the generative stage, is expressed as the time derivative of the temperature sum, and is equal to the instantaneous temperature (normalised to allow for the expression of the temperature sum as °C d):

$$\dot{TS}_{Can} = \frac{1}{86400} T_{Can} \quad [^{\circ}C] \tag{1}$$

where T_{Can} is the simulated canopy temperature. In this model we set TS_{Can} to 0 °C d at the start of the generative period (i.e. the first fruit set). This means that the initial value of TS_{Can} is negative and will stay negative whilst the plant is vegetative. When TS_{Can} exceeds 0 °C d, the carbohydrate distribution to the fruits increases linearly from zero till its full potential is reached at the temperature sum TS_{End}^{Sum}. At values higher than TS_{End}^{Sum}, the carbohydrate distribution to the fruits remains at its potential value.

The evolution of the carbohydrates in the buffer, C_{Buf}, in time is described by:

$$\dot{C}_{Buf} = MC_{AirBuf} - MC_{BufFruit} - MC_{BufLeaf} - MC_{BufStem} - MC_{BufAir} \quad \left[mg\ m^{-2}\ s^{-1}\right] \tag{2}$$

where MC_{AirBuf} is the photosynthesis rate, $MC_{BufFruit}$, $MC_{BufLeaf}$, $MC_{BufStem}$ are the carbohydrate flows to fruits, leaves and stems respectively, and MC_{BufAir} is the growth respiration of the plant. During the light period, carbohydrates produced by photosynthesis are stored in the buffer and, whenever

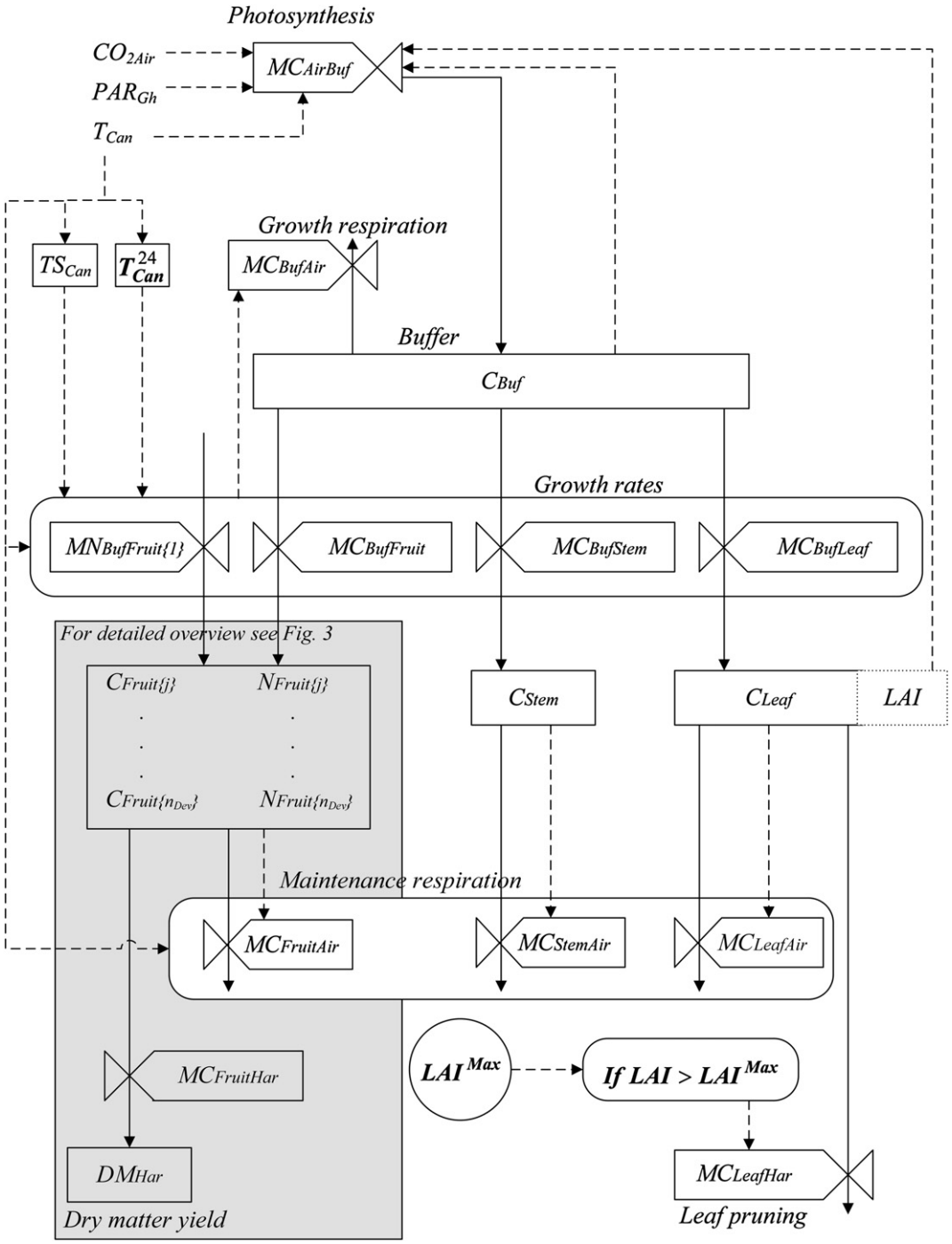

Fig. 2 – Schematic diagram of the tomato yield model using a modelling formalism of Forrester (1962). The boxes represent the state variables of the model, valves are rate variables. The dashed lines are information flows and the solid lines represent mass flows. The box representing the fruit weight, $C_{fruit\{j\}}$, and the number of fruits, $N_{Fruit\{j\}}$, is described in more detail in Fig. 3. The dotted box represents a semi-state variable of the model.

carbohydrates are available in the buffer, carbohydrates flow to the plant organs. This carbohydrate flow stops when the buffer approaches its lower limit. When the buffer approaches its upper limit, further carbohydrates cannot be stored and photosynthesis will be inhibited.

The time between fruit set and fruit harvest is the fruit growth period which is modelled using a "fixed boxcar train" method of Leffelaar and Ferrari (1989). This method implies that carbohydrates and the number of fruits flow from one fruit development stage to the next with a specific development rate (Fig. 3).

When the temperature sum of the plant reaches 0 °C d, the plant shifts from the vegetative stage to the generative stage and carbohydrates are stored in the fruit development stage *j*:

$$\dot{C}_{Fruit\{j\}} = MC_{BufFruit\{j\}} + MC_{Fruit\{j-1\}Fruit\{j\}} - MC_{Fruit\{j\}Fruit\{j+1\}} - MC_{FruitAir\{j\}} \text{ with } j = 1,2\ldots n_{Dev} \quad \left[\text{mg m}^{-2}\text{ s}^{-1}\right] \tag{3}$$

where $MC_{BufFruit\{j\}}$ is the carbohydrate flow from the buffer to fruit development stage j, $MC_{Fruit\{j-1\}Fruit\{j\}}$ and $MC_{Fruit\{j\}Fruit\{j+1\}}$ represent the carbohydrate inflow from the previous development stage and the outflow to the next stage respectively, $MC_{FruitAir\{j\}}$ is the fruit maintenance respiration of development stage j, and n_{Dev} is the total number of fruit development stages. For the first fruit development stage, the carbohydrate inflow from the previous stage is zero. For the last development stage, the carbohydrate outflow to the next stage is described by $MC_{FruitHar}$.

The number of fruits in the fruit development stage j, $N_{Fruit\{j\}}$, affects the carbohydrate distribution to the fruits and is therefore described by:

$$\dot{N}_{Fruit\{j\}} = MN_{Fruit\{j-1\}Fruit\{j\}} - MN_{Fruit\{j\}Fruit\{j+1\}}, \quad j = 1,2\ldots n_{Dev} \quad \left[\text{fruits m}^{-2}\text{s}^{-1}\right] \tag{4}$$

where $MN_{Fruit\{j-1\}Fruit\{j\}}$ is the fruit number flow from fruit development stage $j-1$ to stage j and $MN_{Fruit\{j\}Fruit\{j+1\}}$ is the fruit number flow from fruit development stage j to stage $j+1$. For the first fruit development stage $MN_{Fruit\{j-1\}Fruit\{j\}}$ is replaced by $MN_{BufFruit\{1\}}$. The fruit number flow to the first fruit development stage depends on carbohydrates available for fruit growth and on the truss appearance rate.

The carbohydrates stored in the leaves, C_{Leaf}, are described by:

$$\dot{C}_{Leaf} = MC_{BufLeaf} - MC_{LeafAir} - MC_{LeafHar} \quad \left[\text{mg m}^{-2}\text{ s}^{-1}\right] \tag{5}$$

where $MC_{BufLeaf}$ is the carbohydrate flow from the buffer to leaves, $MC_{LeafAir}$ is the maintenance respiration of the leaves and $MC_{LeafHar}$ is the leaf pruning. The LAI is a semi-state of the model and is calculated by:

$$LAI = SLA \cdot C_{Leaf} \quad \left[\text{m}^2\{\text{leaf}\}\text{m}^{-2}\right] \tag{6}$$

where SLA is the specific leaf area (m^2 {leaf} mg^{-1} {CH_2O}).

The carbohydrates stored in the stem and roots, C_{Stem}, are described by:

$$\dot{C}_{Stem} = MC_{BufStem} - MC_{StemAir} \quad \left[\text{mg m}^{-2}\text{ s}^{-1}\right] \tag{7}$$

where $MC_{BufStem}$ is the carbohydrate flow from the buffer to stems and roots, $MC_{StemAir}$ is the maintenance respiration of the stems and roots.

For simplicity, a continuous harvest rate was assumed. Consequently, the accumulated harvested tomato dry matter (DM), DM_{Har}, equals the outflow of dry matter from the last fruit development stage and is described by:

$$\dot{DM}_{Har} = \eta_{C\_DM} \cdot MC_{FruitHar} \quad \left[\text{mg}\{\text{DM}\}\text{m}^{-2}\text{ s}^{-1}\right] \tag{8}$$

Since all the carbohydrates leaving the carbohydrate buffer are dry matter equivalents, the conversion factor from carbohydrates to dry matter, η_{C_DM}, was obviously 1 mg {DM} mg^{-1} {CH_2O}.

The 24 h mean canopy temperature was approximated by a first order differential equation:

$$\dot{T}^{24}_{Can} = \frac{1}{\tau}\left(kT_{Can} - T^{24}_{Can}\right) \quad \left[^{\circ}\text{C s}^{-1}\right] \tag{9}$$

where τ, represents the time constant of the process and k is the gain of the process. When integrated in the model-based design method, the greenhouse climate model calculates the canopy temperature as a state variable. Therefore, the canopy temperature and the 24 h mean canopy temperature could not be calculated beforehand. To approximate the 24 h mean canopy, the first order approach of Eq. (9) as derived in Appendix A of the e-appendix was incorporated into the model.

3.4. The carbohydrate flow to the individual plant organs

The carbohydrate flow from buffer to the fruits is determined by multiplying the potential fruit growth coefficient rg_{Fruit} by the inhibition factors h:

$$MC_{BufFruit} = h^{MC_{BufOrg}}_{C_{Buf}} \cdot h_{Tcan} \cdot h_{Tcan24} \cdot h_{TcanSum} \cdot g_{Tcan24} \cdot rg_{Fruit} \quad \left[\text{mg m}^{-2}\text{ s}^{-1}\right] \tag{10}$$

where the inhibition factors ($0 < h < 1$): are: $h^{MC_{BufOrg}}_{C_{Buf}}$ (–), insufficient carbohydrates in the buffer; h_{Tcan} (–), non-optimal instantaneous temperature; h_{Tcan24} (–), non-optimal 24 h mean canopy temperatures; and $h_{TcanSum}$ (–), crop development stage. The effect of the 24 h mean temperature on the carbohydrate flow to fruits is described by g_{Tcan24} (–) and rg_{Fruit} (mg {CH_2O} m^{-2} s^{-1}) is the potential fruit growth rate coefficient at 20 °C. The potential fruit growth rate coefficient was determined using the Gompertz growth rate equation with parameter values obtained by De Koning (1994) which resulted in 0.328 mg {CH_2O} m^{-2} s^{-1}. See Appendix C of the e-appendix for a detailed description of the derivation of the potential organ growth rate coefficients. The potential fruit growth rate will only be obtained if: a) sufficient carbohydrates are available in the carbohydrate buffer, which in turn depends of the photosynthesis rate; b) the temperature is optimal and c) the plant is fully generative.

The carbohydrates available for fruit growth (Eq. (10)) are distributed to the different fruit development stages. The carbohydrate flow to the first fruit development stage depends on fruit set (Fig. 3 and Eq. (35) in the e-appendix) and has preference over the remaining fruit development stages because, at relatively low carbohydrate availability, the plant will give priority to fruit set. The remaining carbohydrates are distributed to the remaining fruit development stages. Each of these carbohydrate flows depends on the number of fruits in the specific fruit development stage and on the growth rate of each fruit as function of fruit development stage (Fig. 3 and Eq. (36) in the e-appendix). Under conditions of carbohydrate shortage in the buffer, all fruit development stages (except the first one) will then equally share in carbohydrate shortage.

The carbohydrate flow from buffer to the leaves and stem is described by:

$$MC_{BufOrg(i)} = h^{MC_{BufOrg}}_{C_{Buf}} \cdot h_{Tcan24} \cdot g_{Tcan24} \cdot rg_{Org(i)} \quad i = 2,3 \quad \left[\text{mg m}^{-2}\text{ s}^{-1}\right] \tag{11}$$

where i represents the plant organ code for Leaf and Stem, and $rg_{Org(i)}$ is the potential organ growth rate coefficient at 20 °C. The potential vegetative growth rate coefficients were based

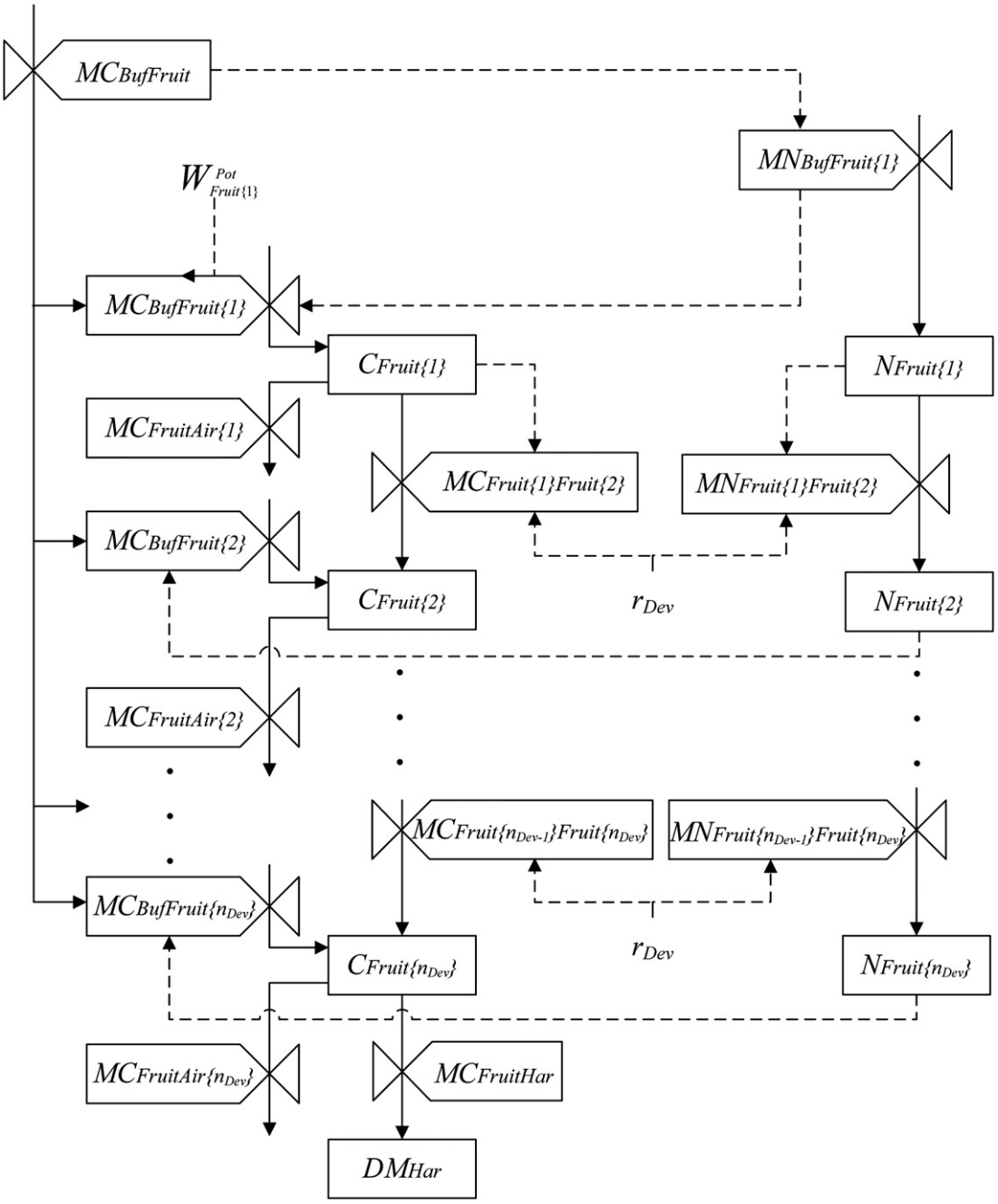

Fig. 3 – Fruit development is modelled by describing for each fruit development stage the number of fruits, $N_{Fruit\{j\}}$ and the amount of carbohydrates, $C_{Fruit\{j\}}$. As in Fig. 2, the boxes represent the state variables of the model, valves are rate variables. The dashed lines are information flows and the solid lines represent the carbon and fruit flows. The carbohydrates available for fruit growth, $MC_{BufFruit}$, are distributed to the different fruit development stages $C_{Fruit\{j\}}$. The carbohydrate flow to the first development stage $MC_{BufFruit\{1\}}$ is affected by the fruit set $MN_{BufFruit\{1\}}$ which in turn is influenced by the carbohydrates available for fruit growth $MC_{BufFruit}$ and the potential fruit growth rate $W^{Pot}_{Fruit\{1\}}$ (Eq. (35) in e-appendix). The carbohydrate flow to the remaining fruit development stages is influenced by the available carbohydrates $MC_{BufFruit}$, the number of fruits $N_{Fruit\{j\}}$ and by a development stage dependent fruit growth rate (Eq. (36) in the e-appendix).

on the carbohydrate distribution to different plant organs as described by Heuvelink (1996) and on the potential fruit growth rate coefficient, which resulted in rg_{Leaf} of 0.095 mg $\{CH_2O\}$ m^{-2} s^{-1} and rg_{Stem} of 0.074 mg $\{CH_2O\}$ m^{-2} s^{-1}. In agreement with Table 1, these carbohydrate flows are not influenced by instantaneous temperature. The two lumped temperature-dependent growth inhibition functions of Eqs. (10) and (11) are described in more detail in this section.

The literature review revealed that crop growth was inhibited by non-optimal levels of the instantaneous and 24 h mean temperature and this was described by two trapezoid growth inhibition functions, h_{Tcan} and h_{Tcan24}, respectively.

Each inhibition function was based on Boote and Scholberg (2006) and was described by four cardinal temperatures (Fig. 4). Below a certain base temperature T_{Base} no carbohydrate flow to organs is expected ($h = 0$), between T_{Opt1} and T_{Opt2} the carbon flow is maximal ($h = 1$) and above T_{Max} no carbohydrate flow is expected ($h = 0$). Between T_{Base} and T_{Opt1} and between T_{Opt2} and T_{Max} a linear relationship between inhibition and temperature is assumed. The growth inhibition function of Boote and Scholberg (2006) is not differentiable and therefore not suitable for dynamic optimisation purposes. Therefore, the non-differentiable inhibition functions were each smoothed by multiplying two smoothed conditional "if/else" statements as described in Appendix B of the e-appendix. The cardinal temperatures were determined based on values presented in Table 1. The derivation of these temperatures is described in the e-appendix.

4. Model validation

For all four temperature regimes, the yield model was validated using the same model parameters (Table 4). The model was first validated for mild temperatures commonly encountered under Dutch greenhouse conditions and second for extreme temperatures encountered under southeast Spanish greenhouse conditions. Third, the model was validated for non-optimal temperature conditions. Fourth, the tomato harvest rate for long-term diurnal temperature oscillations was determined and compared with data obtained from literature.

To simulate crop yield, the differential equations were solved with an ODE solver of Matlab 7.1®. Hourly greenhouse climate data, i.e. greenhouse air temperature, CO_2-concentration and outside global radiation were used as model inputs. Since the canopy temperature was not measured, it was assumed to be equal to the greenhouse air temperature. An overview of the data needed to run the model for the Dutch and Spanish greenhouses is presented in Table 5.

All model parameters were taken from literature, with two exceptions. For the Dutch and Spanish validation studies, the LAI was measured as initial crop condition. And the initial leaf carbohydrates were calculated based on the LAI and the specific leaf area (Eq. (6)). The initial stem and root carbohydrates were determined by multiplying the leaf carbohydrates by a ratio that depends on the vegetative development. The initial temperature sum was unknown for the Spanish studies and for the constant temperature experiments conducted by Adams et al. (2001). This parameter was fitted to the data to ensure that the moment of the simulated first fruit set was equal to the measured first fruit set. Therefore, all simulations presented in Figs. 6–8 can be considered as model validations, at least from the first fruit set onwards.

4.1. Model validation for mild temperature conditions

The model was validated with measured tomato yield – obtained under mild temperature conditions – of two Dutch greenhouse growers in different production years. In both cases tomatoes were grown in a Venlo-type greenhouse which was equipped with CO_2-enrichment and a heating system. Tomatoes were grown close to the optimal 24 h mean canopy temperature interval of 18–22 °C with varying CO_2-concentrations and PAR levels commonly encountered in Dutch greenhouses (Table 5).

4.2. Model validation for Spanish temperature conditions

The model was validated with measured tomato yield obtained for southern Spanish climate conditions for a low-tech "raspa y amagdo" greenhouse (LT) with only natural ventilation and a high-tech greenhouse arch shape multi-tunnel (HT) equipped with natural ventilation, a heating system, a thermal screen, an external shade screen, a fogging system and CO_2 enrichment. In the LT greenhouse tomatoes were exposed to strongly fluctuating temperatures being frequently non-optimal (Table 5). In contrast, in the HT greenhouse tomatoes were grown closer to the optimal 24 h mean canopy temperature interval. Since both simulations started in the

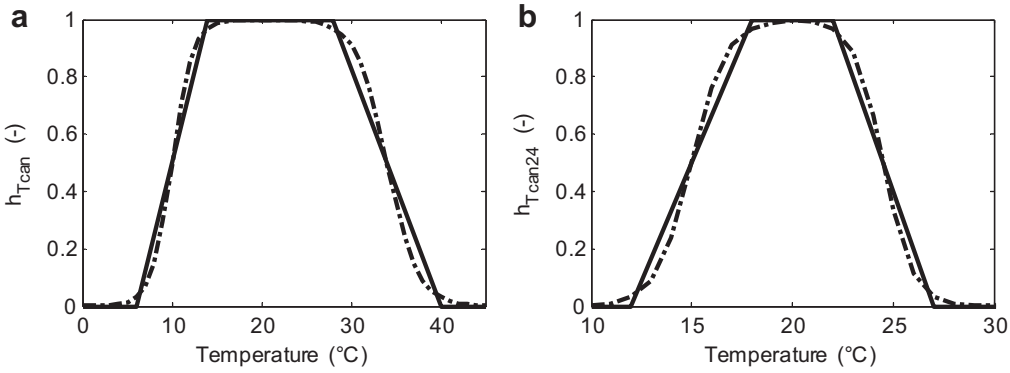

Fig. 4 – The growth inhibition by the instantaneous temperature (a) and by the 24 h mean canopy temperature (b). The solid lines represent the non-differentiable inhibition functions and the dashed dotted lines represent the differentiable inhibition functions. The non-differentiable inhibition functions were each smoothed by multiplying two smoothed conditional "if/else" statements as described in appendix B of the Electronic appendix. The cardinal temperatures for both inhibition functions are presented in Table 4.

Table 5 – The location, crop production data, initial conditions, the mean greenhouse climate conditions for the Dutch growers A and B and for the low-tech and high-tech located in southern Spain. The values between the brackets represent the standard deviation. Some initial crop conditions were not measured but calculated as described in section 4.

	Grower A	Grower B	Low-tech Spain	High-tech Spain
Location				
Latitude	52°0'N	52°0'N	36°57'N	36°48'N
Longitude	4°3'E	4°3'E	2°00'W	2.43'W
Elevation (m)	−3	−3	180	151
Crop production data				
Start growing cycle	10-12-1999	8-12-1997	1-8-2009	26-9-2003
End growing cycle	2-10-2000	23-9-1998	5-05-2010	9-07-2004
Cultivar	Aromata	Rapsodie	Atletico	Pitenza
Greenhouse transmission	78%	78%	55%	40%
LAI^{Max}	3.0	2.85	3.5	3.5
Initial conditions				
Start simulation	6-1-2000, start of generative stage	6-1-1998, start of generative phase	1-8-2009	26-9-2003
TS^{Sum}_{Can0} (°C d)	0	0	−900	−650
LAI_0 ($m^2\ m^{-2}$)	1.06	1.25	0.4	0.1
C_{Leaf0} (mg {CH_2O} m^{-2})	40×10^3	47×10^3	15×10^3	3.8×10^3
C_{Stem0} (mg {CH_2O} m^{-2})	30×10^3	31×10^3	15×10^3	3.8×10^3
Indoor climate				
Mean canopy temperature (°C)	18.2 (2.7)	19.1 (2.1)	17.5 (7.0)	19.7 (3.2)
Daily global outside radiation (MJ m^{-2} day^{-1})	12.2 (7.4)	9.7 (5.6)	12.9 (5.6)	15.9 (7.7)
Mean CO_2-concentration at daylight (μmol mol^{-1})	677 (301)	659 (253)	355 (15)	476 (81)

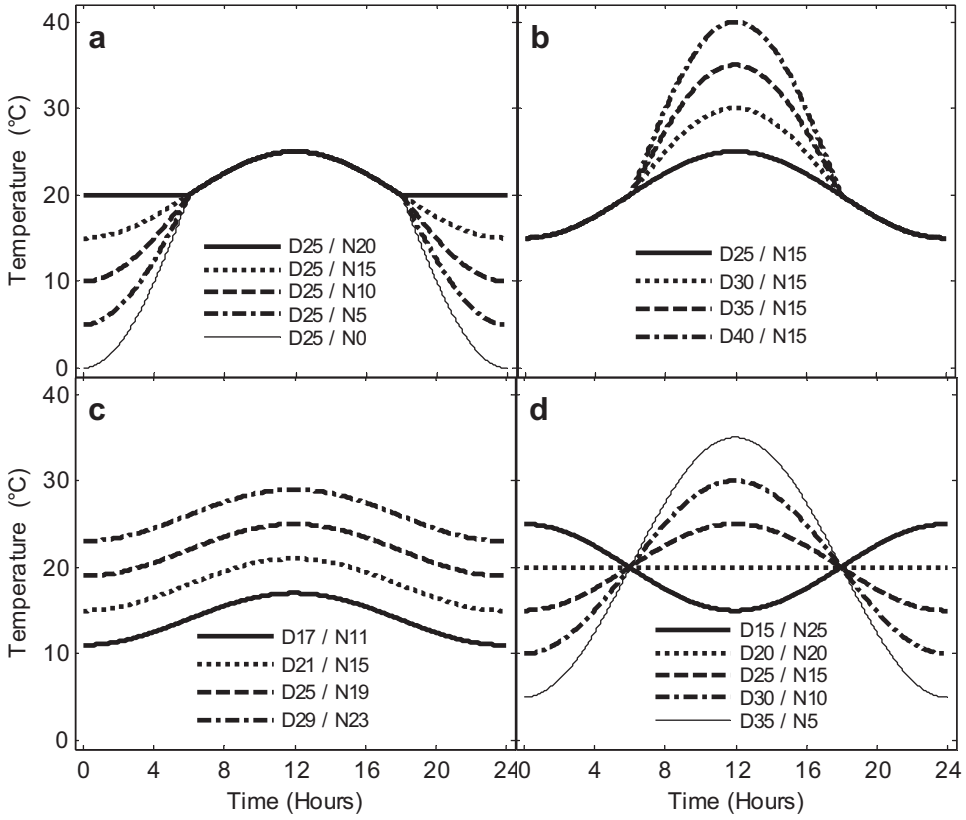

Fig. 5 – The temperature trajectories for the four temperature sensitivity studies: a) different night temperatures (T_{night}); b) different high day temperatures (T_{day}); c) different mean temperatures (T_{mean}); and d) difference between day and night temperature (T_{DIF}).

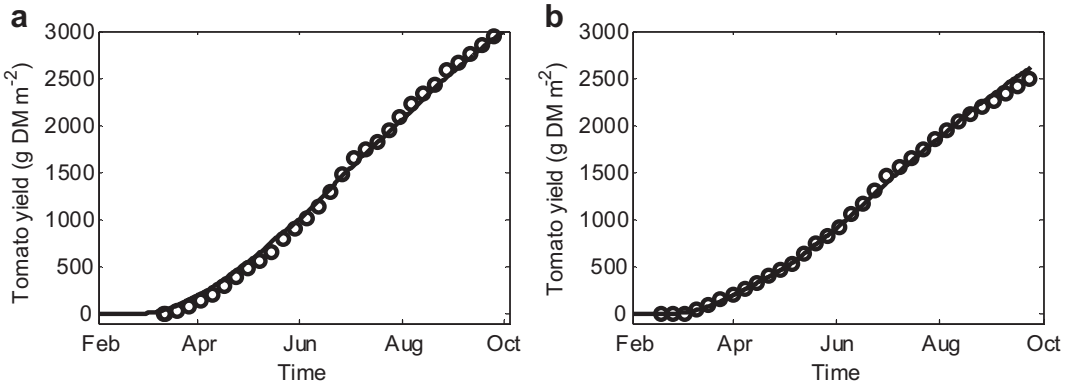

Fig. 6 – The simulated tomato yield compared with measurements for grower A (a) and for grower B (b) under mild temperatures in Dutch greenhouses. Solid lines represent the simulations and the circles represent the measurements.

vegetative stage, negative values for the mean temperature sum at the start of the simulation were estimated.

4.3. *Model validation for extreme temperature conditions*

The simulated tomato yield for four different mean temperature levels was compared with yield measurements of the cultivar Liberto conducted in growth chambers by Adams et al. (2001). Until 26 weeks after sowing, Adams et al. (2001) determined the yield for four constant temperature regimes of 14 °C, 18 °C, 22 °C and 26 °C with the following climate set-points: a daylight period of 12 h with 315 μmol photons m^{-2} s^{-1} PAR above the canopy and a CO_2-concentration of 1000 μmol CO_2 mol^{-1} air. The model simulated tomato yield using the climate set-points of Adams as model inputs.

The simulated temperature treatment started similarly to Adams et al. (2001) – 21 days after sowing – when plants were still in the vegetative stage. Since destructive crop measurements were not performed, the following initial conditions were estimated for the 21 days old tomato crop: LAI_0 was 0.1, C_{Leaf0} was 3.8×10^3 mg {CH_2O} m^{-2}, C_{Stem0} was 2.5×10^3 mg {CH_2O} m^{-2}. Since the generative stage was assumed to start after a fixed temperature sum, the same initial temperature sum, T^{Sum}_{Can0}, of −550 °C d was used for all four simulations. This initial temperature sum was the average value of the four temperature sums needed to simulate first fruit set in agreement with the measured first fruit set. As a best estimate of LAI^{Max}, the mean of the measured LAI (2.5) of a full grown commercial tomato crop was used.

To make a fair comparison between the measured and simulated crop yield results, the measured fresh tomato yield per plant obtained by Adams et al. (2001) was expressed in dry matter tomato yield (g {DM} m^{-2}). For this re-calculation, the plant density of each growth chamber was set to 2.2 plants m^{-2} and the average dry matter content of the fruits for the treatments 14 °C, 18 °C, 22 °C and 26 °C were set at 10.7%, 6.2%, 5.6% and 6.2%, respectively according to Adams (personal communication, 2008).

4.4. *Model evaluation of effects of diurnal temperature oscillations*

The effect of diurnal temperature oscillations on crop yield was investigated for four temperature trajectories, namely: low night temperatures (T_{night}), high day temperatures (T_{day}), mean temperature (T_{mean}) and the difference between day and night temperature (DIF) (T_{DIF}) as shown in Fig. 5. The temperature trajectories of T_{night}, T_{day} and T_{DIF} were described by a sine function with a mean temperature of 20 °C and

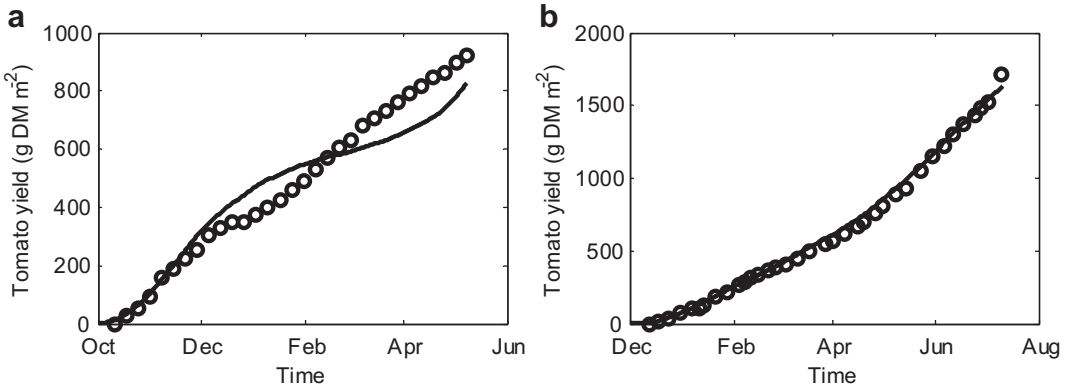

Fig. 7 – The simulated tomato yield compared with measurements in a low-tech greenhouse (a) and a high-tech greenhouse (b) located in South Spain. Solid lines represent the simulations and the circles represent the measurements.

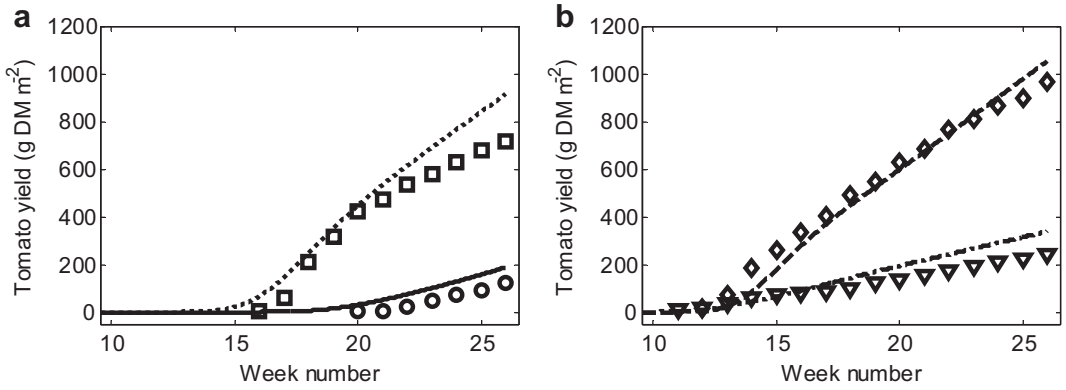

Fig. 8 – The simulated tomato yield for four different mean temperature treatments between week number 10 and 26 after sowing. (a) presents the crop yield at 14 °C (solid line represents the simulation and circles the measurements) and at 18 °C (dotted line represents the simulation and squares the measurements). (b) presents the crop yield at 22 °C (dashed line represents the simulation and diamonds the measurements) and at 26 °C (dashed dotted line represents the simulation and triangles the measurements). Source of the measured data was Adams et al. (2001).

a different day and night amplitude. The temperature trajectory of T_{mean}, was described by a variable mean temperature (14 °C, 18 °C, 22 °C and 26 °C) with a fixed day and night amplitude of 3 °C.

The tomato harvest rate for the four temperature scenarios was simulated under the following conditions: the plant was totally in the generative stage with a LAI^{Max} of 2.5 and the simulation period was 100 days. The PAR absorbed by the crop during the light period of 12 h was described by a sinusoidal function. To investigate how the harvest rate response to temperature depends on PAR, two PAR amplitudes were used: 460 μmol photons m^{-2} s^{-1} and 920 μmol photons s^{-1} m^{-2}. The CO_2 level in the greenhouse was 370 μmol CO_2 mol^{-1} air. The tomato harvest rates were determined for the last seven days of the total production period of 100 days to decrease the influence of the initial conditions on the results.

5. Results and discussion

In Section 5.1–5.4 the validation results are presented and discussed with respect to model performance for the tomato yield (g {DM} m^{-2}). In Section 5.5 the model is discussed with respect to other tomato yield models, and relevant yield model aspects for greenhouse design optimisation are discussed as well. All tomato yield simulations were performed with the same set of model parameters.

5.1. *Model validation for mild temperature conditions*

For two commercial Dutch greenhouses, with mild temperature conditions and varying global radiation levels and CO_2-concentrations (Table 5), the model simulated the tomato yield very well (Fig. 6). Only the tomato yield of grower B was slightly overestimated at the end of the production period. The higher crop yield of greenhouse A compared to greenhouse B was caused by its higher external global radiation.

5.2. *Model validation for southern Spanish temperature conditions*

The impact of non-optimal temperatures on model performance was evaluated using southern Spanish climate conditions. The tomato yield of the LT greenhouse was simulated with fair accuracy (Fig. 7a). The cumulative measured tomato yield of 922 g {DM} m^{-2} was underestimated by the model by 97 g {DM} m^{-2}. This difference will not be a problem for greenhouse design because this error is within the uncertainty of the model. The trend of the simulated yield differed from the measured yield which might be caused by errors introduced due to the conversion from measured tomato fresh tomato yield to calculated dry matter yield. For this conversion, a constant dry matter content (DMC) was used since time variant measurements were missing. However, according to Segura, Contreras, Salinas, and Lao (2009) the dry matter content varies along the production period with a relatively low DMC in winter and a relatively high DMC in summer under south Spanish conditions. Using a time dependent DMC would improve the trend of the measured dry matter yield. Additionally, the underestimation of the measured crop yield might be caused by applying generic cardinal temperatures for the growth inhibition functions to a cultivar bred to withstand low temperatures. To improve the simulation result further, an option is to calibrate these cardinal temperatures for each cultivar.

For the HT greenhouse, the model predicted accurately the tomato yield (Fig. 7b). Only at the end of the production period the crop yield was underestimated slightly because of the way dry matter outflow from the last fruit development stage due to harvest was simulated (Eq. (8)), whereas in practice all marketable tomatoes on the plant were harvested.

5.3. *Model validation for extreme temperature conditions*

Comparing simulated fruit yield with yield measured by Adams et al. (2001), it can be observed that the model

simulated with fair accuracy the effect of the mean temperature regimes of 14 °C, 18 °C, 22 °C and 26 °C on fruit yield (Fig. 8a, b). The model correctly captured a reduction in yield at non-optimal mean temperatures of 14 °C and 26 °C. Specifically, the simulated relative decrease in fruit yield at non-optimal temperatures was almost equal to the measured relative reduction in yield (Table 6) as caused by the growth inhibition due to temperature (Eq. (10) and Fig. 4). However, the model tended to overestimate the yield at the end of the growing period by on average 33% (Table 6). This overestimation might be caused by growth chamber conditions not equal to those in the greenhouse for which the model was developed.

Temperature effects on first fruit harvest were simulated in close agreement to the measured first fruit harvest. Specifically, low mean temperature resulted in a delayed simulated first fruit harvest which was caused by the temperature effect on both vegetative development rate and generative development rate. However, for low mean temperatures (14 °C and 18 °C) the simulated first fruit harvest was earlier than the measured first fruit harvest whereas for high mean temperatures (22 °C and 26 °C) the simulated first fruit harvest was later than the measured values. The simulated timing of first fruit harvest at 14 °C and 26 °C differed by 5 weeks whereas 10 weeks were measured. This underestimation was caused by processes both in the vegetative and the fruit growth period as explained hereafter.

Regarding vegetative development, a linear relationship with temperature was modelled. However, measurements indicated that at sub-optimal temperatures the crop needs a higher temperature sum to fulfil the vegetative development period (Adams, personal communication 2009). To improve the simulation of the vegetative period, a base temperature should be introduced in the temperature sum description of Eq. (1).

The fruit growth period was simulated based on parameters for temperature sum for fruit development from De Koning (1994) as described in Eq. (32) of the Electronic appendix, being different from those Adams et al. (2001) for the measurements under consideration. The underestimation of the fruit growth period at lower temperatures is due to the lower temperature sum from De Koning (1994) which resulted in a 24 days shorter growing period at 14 °C than the observed fruit growth period of Adams et al. (2001).

Table 6 – Simulated and measured production values for four temperature treatments.

	Temperature (°C)			
	14	18	22	26
Production (g {DM} m^{-2})				
Measured	123	720	970	241
Simulated	188	919	1057	340
Relative production compared to maximum (%)				
Measured	13	74	100	25
Simulated	18	87	100	32
Final production difference between simulations and measurements (%)	53	28	9	41

5.4. *Model evaluation for diurnal temperature oscillations*

To evaluate the model for its response to diurnal temperature oscillations, the trends of the simulated crop harvest responses to four extreme temperature treatments (Figs. 5 and 9) were compared with harvest responses obtained from literature (Table 1).

The impact of a low night temperature on harvest rate (Fig. 9a) shows that the model reproduced the expected interaction between radiation and temperature on harvest rate. In agreement with Martínez Mirón (2008) the optimum night temperature increased with increasing PAR level. Specifically, at a low PAR level the optimum night temperature was 5 °C whereas at a high PAR level the optimum night temperature was 10–15 °C. In addition, the positive impact of PAR on harvest rate at moderate temperature trajectories was demonstrated. For instance, for the day/night treatment of 25 °C/15 °C, the harvest rate at a low PAR level was 55.2% of the harvest rate at a high PAR level (123.1 g m^{-2} $week^{-1}$).

Although negative effects of low night temperatures on tomato harvest rate were incorporated in the model, at low PAR levels the simulated tomato harvest rate increased slightly with decreasing night temperature. This result was in agreement with Martínez Mirón (2008) who measured, under constant shading in the autumn and winter season in southern Spain, a higher yield at a mean night-time temperature of 13.2 °C than at 15.2 °C. This effect was caused by lower maintenance respiration losses at low night temperature. It seems that the model was not valid for extremely low night temperatures because at 0 °C and 5 °C still a reasonable crop yield was simulated. This overestimation was caused by not modelling lethal damage or hormonal imbalances at low temperature.

Fig. 9b shows that too high day temperatures lowered the harvest rate for both PAR levels. Under high PAR levels, the harvest rate at a maximum day temperature of 40 °C was 54.5% of the harvest rate at a maximum day temperature of 25 °C. A similar trend was observed by Zhang et al. (2008) who measured a tomato yield decrease of 46.1% at 35 °C compared to 25 °C.

In agreement with the crop yield measurements of Adams et al. (2001), Fig. 9c shows that non-optimal mean temperature affected the harvest rate negatively at both PAR levels. Specifically, the harvest rate under high PAR levels at a mean temperature of 14 °C was 32.0% of the harvest rate at the mean temperature of 18 °C (129.1 g m^{-2} $week^{-1}$) whereas the harvest rate at a mean temperature of 26 °C was 19.6% of the harvest rate at the mean temperature of 18 °C. These results agreed well with crop yield reductions at non-optimal mean temperatures shown in Table 1. The tomato harvest rate at non-optimal mean temperatures was equal for both PAR levels. Specifically, at non-optimal temperatures the carbon outflow from buffer to fruits was reduced due to the temperature-dependent growth inhibition functions (Eq. (10) and Fig. 4) whereas the inflow of carbon produced by photosynthesis sustained until buffer saturation. At buffer saturation, the photosynthesis was inhibited which resulted in lower crop yield values. Thus temperature not PAR was the limiting factor for crop growth.

A DIF lower than 20 °C influenced the harvest rate only slightly (Fig. 9d) which was in close agreement with

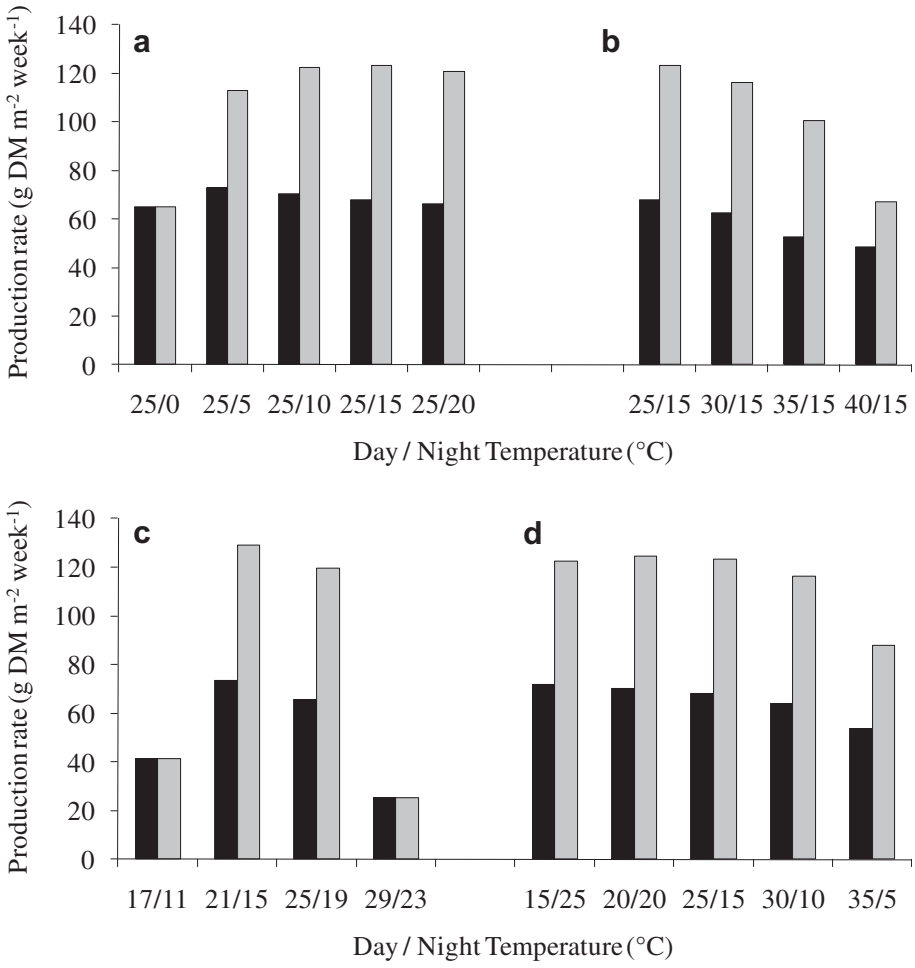

Fig. 9 – The effect of daily temperature fluctuations on production rate for two levels of PAR: 460 μmol photons m^{-2} {greenhouse} s^{-1} (the black bar) and 920 μmol photons m^{-2} {greenhouse} s^{-1} (the grey bar). The crop production sensitivity to the following temperature treatments was determined: a) the night temperature (T_{night}); b) the day temperature (T_{day}); c) the 24 h mean temperature (T_{mean}); and d) the difference between day and night temperature (T_{DIF}).

Mavrogianopoulos and Kyritis (1989) who found a similar crop yield at a DIF of 6 °C and 18 °C. In contrast, a large DIF of 30 °C did negatively affect the crop harvest rate. Specifically, for high PAR levels, the treatment of 35/5 °C resulted in 70.5% of the harvest rate obtained in the treatment of 20/20 °C (124.4 g m^{-2} $week^{-1}$). The simulated harvest reduction was caused by both a sub-optimal night temperature of 5 °C and a supra-optimal day temperature of 35 °C. Although the effect of an extremely high DIF on tomato harvest rate was not explicitly described by the model, its impact on tomato harvest rate was properly simulated.

5.5. *Discussion of model performance in view of greenhouse design*

In horticultural research a considerable number of tomato yield models have been developed. For the aim of greenhouse design optimisation, the presented yield model has two advantages compared to, for example, the TOMGRO model (Dayan et al., 1993; Jones et al., 1991): 1) the crop response to extreme values of both instantaneous and diurnal mean temperature effects are modelled implying that the model can be used within a model-based greenhouse design method, 2) the model is described in differential equations with continuous differentiable right-hand sides enabling us to combine the yield model with the greenhouse climate model developed by Vanthoor et al. (2011) to solve differential equations with an existing ordinary differential equation solver and to use gradient-based-optimisation algorithms to optimise greenhouse design. Furthermore, the model describes, based on crop physiological processes, the most important effects of extreme temperatures on tomato yield. These crop physiological processes were lacking in related studies. Specifically, Ioslovich and Seginer (1998) bounded the minimum and maximum temperature and Ooteghem (2007) penalised extreme temperatures by introducing a term in the cost criterion.

Given these results, obtained for a broad range of temperature conditions, the model is considered to be sufficiently accurate to be used for developing a model-based greenhouse design method. However, since our aim was to develop a design method that focussed on the optimisation of a set of

design elements, model aspects that might be relevant may have been neglected or oversimplified. Therefore, whenever better or new modules are available, they can be easily incorporated into the design method. Some issues that might improve the generality of the model-based design method are discussed in more detail here.

To enhance the generality, yield models of other crops than tomatoes should be developed that fulfil the same requirements as demanded of the tomato yield model. Additionally, the transpiration module of the greenhouse climate model of Vanthoor et al. (2011) should then be adjusted to this crop as well. Performance of the tomato yield model might be improved by describing the impact of temperature and other climate variables on each growth and development process such as fruit set, fruit abortion and membrane integrity. Since modules for these processes were not available, two lumped temperature-dependent growth inhibition functions were used in this study. Growth inhibition functions were based on literature values and therefore photosynthesis effects might have been captured in these functions. Since the simulated photosynthesis depended already on temperature, effects of non-optimal temperatures on photosynthesis might have been overestimated by the model. However, first analysis of the crop yield prediction for non-optimal temperature conditions revealed that the incorporation of photosynthesis effects in the inhibition functions did not play an important role as can be seen in Figs. 8 and 9 due to the plant's ability to store carbohydrates in the buffer.

To solve a greenhouse design problem, the economic benefits of crop yield must be determined. Since the presented model described dry matter yield as a function of greenhouse climate, the impact of dry matter content on fresh tomato yield should be integrated into the model. In addition, this DMC should then be described as a function of electrical conductivity of the growing medium, on outdoor climate variations (Segura et al., 2009) and on non-optimal temperatures (Adams et al., 2001).

Subsequently, the quality of the tomatoes must be incorporated into the model since they determine the economic value of the yield. According to Adams et al. (2001) the quality of the tomatoes and marketable ratio depends on temperature and air humidity. Therefore, when using the model for optimal greenhouse design, it would be better to describe the impact of humidity on quality and yield. To do this, the tomato quality model of Liu, Génard, Guichard, and Bertin (2007) can be used as a starting point. No direct effects of a large VPD on photosynthesis were modelled. However, when integrated in the model-based design method, a large VPD will indirectly affect growth through its effect on transpiration and canopy temperature. Additionally, fertigation was assumed to be non-limiting for crop growth whereas in practice it might occasionally be non-optimal. The impact of fertigation on crop yield can be described by the nutrient model of Van Straten, Vanthoor, Van Willigenburg, and Elings (2006).

Since temperature effects on crop yield are cultivar-dependent (Adams et al., 2001; Camejo et al., 2005; De Koning, 1994; Khayat et al., 1985), the model performance can be improved by calibration of the parameters related to the growth inhibition functions, photosynthesis functions and fruit growth period. Furthermore, instead of using a constant SLA, a seasonal dependent SLA based on Heuvelink (1996) might improve the model performance. Additionally, the estimation of the vegetative growth period might be improved by introducing a non-zero base temperature in the temperature sum calculation. No long term effects of extreme temperatures on crop yield were modelled, whereas in practice extreme temperatures indeed affect crop yield in the long term (Yakir et al., 1986). Consequently, the simulated crop could, erroneously, totally recover from extreme temperatures. To avoid the resulting overestimated yields affecting the greenhouse design optimisation problem, the greenhouse air temperature must not go beyond these extreme temperature values.

6. Conclusion

In this research, a yield model that describes the effect of greenhouse climate on tomato yield was developed and validated. The ultimate aim is to use this model in a model-based method to design greenhouses for the wide variety of climate and economic conditions that can be expected around the world. A literature survey of temperature effects on tomato yield was performed and the main temperature effects were implemented in the crop yield model.

Validation results showed that the model fulfilled the three predefined requirements. Specifically, the model covers the effects of indoor climate and non-optimal temperature conditions on crop yield (requirements 1 and 2). Without calibration of model parameters, the tomato yield model predicted with fair accuracy the tomato yield levels for four temperature regimes. In more detail, the tomato yield was simulated accurately for both near-optimal and non-optimal temperature conditions in the Netherlands and southern Spain respectively, given the varying light levels and CO_2-concentrations. In addition, the adverse effects of extremely low as well as high mean temperatures on tomato yield and timing of first fruit harvest were simulated with fair accuracy. The simulated yield response to extreme diurnal temperature oscillations were in agreement with literature values. Since the presented model consisted of a set of differential equations with continuous differentiable right-hand sides, requirement 3 was fulfilled as well. All model equations are presented in this paper and in the e-appendix to allow others to implement and reproduce our findings.

Given these results, obtained for a broad range of temperature conditions, the model is considered to be sufficiently accurate to be used for developing a model-based greenhouse design method. Therefore, the presented model will be integrated in the design method with the aim to design the best greenhouse design for local climate and economic conditions.

Acknowledgements

We thank "De Gebroeders Duijvestijn BV", Pijnacker, The Netherlands; "Grower Hooymans", Pijnacker, The Netherlands; and Dr Steven Adams, Warwick University, United

Kingdom for providing the crop yield data. For providing the Spanish crop yield data we thank Francisco Belzunces, the nursery Frutas Nijasol with special thanks to Mario and Juan José Magan Cañadas of the experimental station "Las Palmerillas" of Cajamar. We thank Ignacio Rodríguez Gracia, Eduardo Rumí Ronda and Nelleke Koene of HortiMaX España to bring us into contact with the Spanish growers. This research is part of the strategic research programs "Sustainable spatial development of ecosystems, landscapes, seas and regions" and "Sustainable Agriculture" that are funded by the former Dutch Ministry of Agriculture, Nature Conservation and Food Quality. We gratefully acknowledge the editor and reviewers for their constructive comments on earlier versions of this manuscript.

Appendix. Supplementary data

Supplementary data associated with this article can be found, in the online version, at doi:10.1016/j.biosystemseng.2011.08.005.

REFERENCES

Adams, S. R., Cockshull, K. E., & Cave, C. R. J. (2001). Effect of temperature on the growth and development of tomato fruits. *Annals of Botany, 88*(5), 869–877.

Baille, A. (1999). Overview of greenhouse climate control in the mediterranean regions. *Cahiers Options Mediterraneennes, 31*, 59–76.

Baytorun, A. N., Topçu, S., Abak, K., & Daşgan, Y. (1999). Growth and production of tomatoes in greenhouses at different temperature levels. *Gartenbauwissenschaft, 64*(1), 33–39.

Boote, K. J., & Scholberg, J. M. S. (2006). Developing, parameterizing, and testing of dynamic crop growth models for horticultural crops. *Acta Horticulturae, 718*, 23–34.

Brüggemann, W., van der Kooij, T. A. W., & van Hasselt, P. R. (1992). Long-term chilling of young tomato plants under low light and subsequent recovery – I. Growth, development and photosynthesis. *Planta, 186*(2), 172–178.

Camejo, D., Rodríguez, P., Angeles Morales, M., Miguel Dell'Amico, J., Torrecillas, A., & Alarcón, J. J. (2005). High temperature effects on photosynthetic activity of two tomato cultivars with different heat susceptibility. *Journal of Plant Physiology, 162*(3), 281–289.

Criddle, R. S., Smith, B. N., & Hansen, L. D. (1997). A respiration based description of plant growth rate responses to temperature. *Planta, 201*(4), 441–445.

Dayan, E., van Keulen, H., Jones, J. W., Zipori, I., Shmuel, D., & Challa, H. (1993). Development, calibration and validation of a greenhouse tomato growth model: I. Description of the model. *Agricultural Systems, 43*(2), 145–163.

De Koning, A. N. M. (1994). *Development and dry matter distribution in glasshouse tomato: A quantitative approach*. Wageningen: Wageningen University.

De Zwart, H. F. (1996). *Analyzing energy-saving options in greenhouse cultivation using a simulation model*. Wageningen: Wageningen University.

Evans, J. R., & Farquhar, G. D. (1991). Modelling canopy photosynthesis from the biochemistry of the C_3 chloroplast. In K. J. Boote, & R. S. Loomis (Eds.), *Modeling crop photosynthesis - from biochemistry to canopy* (pp. 1–15). Wisconsin, USA: CSSA Madison.

Farquhar, G. D. (1988). Model relating subcellular effects of temperature to whole plant responses. *Symposia of the Society for Experimental Biology, 42*, 395–409.

Farquhar, G. D., Caemmerer, S v, & Berry, J. A. (1980). A biochemical model of photosynthetic CO_2 assimilation in leaves of C_3 species. *Planta, 149*(1), 78–90.

Farquhar, G. D., & von Caemmerer, S. (1982). Modelling of photosynthetic response to environmental conditions. In O. L. Lange, P. S. Nobel, & C. B. Osmond (Eds.), *Physiological plant ecology, water relations and carbon assimilation* (pp. 549–582). Berlin: Springer-Verlag.

Forrester, J. W. (1962). *Industrial dynamics*. Cambridge: MIT Press.

Gent, M. P. N., & Ma, Y. Z. (1998). Diurnal temperature variation of the root and shoot affects yield of greenhouse tomato. *HortScience, 33*(1), 47–51.

Heckathorn, S. A., Downs, C. A., Sharkey, T. D., & Coleman, J. S. (1998). The small, methionine-rich chloroplast heat-shock protein protects photosystem II electron transport during heat stress. *Plant Physiology, 116*(1), 439–444.

Heuvelink, E. (1989). Influence of day and night temperature on the growth of young tomato plants. *Scientia Horticulturae, 38*(1–2), 11–22.

Heuvelink, E. (1996). *Tomato growth and yield: Quantitative analysis and synthesis*. Wageningen: Wageningen University.

Ioslovich, I., & Seginer, I. (1998). Approximate seasonal optimization of the greenhouse environment for a multi-state-variable tomato model. *Transactions of the American Society of Agricultural Engineers, 41*(4), 1139–1149.

Jones, J. W., Dayan, E., Allen, L. H., Van Keulen, H., & Challa, H. (1991). Dynamic tomato growth and yield model (TOMGRO). *Transactions of the American Society of Agricultural Engineers, 34*(2), 663–672.

Khayat, E., Ravad, D., & Zieslin, N. (1985). The effects of various night-temperature regimes on the vegetative growth and fruit production of tomato plants. *Scientia Horticulturae, 27*(1–2), 9–13.

Leffelaar, P. A., & Ferrari, T. J. (1989). Some elements of dynamic simulation. In R. Rabbinge, S. A. Ward, & H. H. van Laar (Eds.), *Simulation and systems management in crop protection* (pp. 19–45). Wageningen: Pudoc.

Linker, R., Seginer, I., & Buwalda, F. (2004). Description and calibration of a dynamic model for lettuce grown in a nitrate-limiting environment. *Mathematical and Computer Modelling, 40*(9–10), 1009–1024.

Liu, H. F., Génard, M., Guichard, S., & Bertin, N. (2007). Model-assisted analysis of tomato fruit growth in relation to carbon and water fluxes. *Journal of Experimental Botany, 58*(13), 3567–3580.

Marcelis, L. F. M., Heuvelink, E., & Goudriaan, J. (1998). Modelling biomass production and yield of horticultural crops: a review. *Scientia Horticulturae, 74*(1–2), 83–111.

Martínez Mirón, A. (2008). *Influencia de la temperatura y de la radiación sobre un cultivo de tomate en invernadero*. Almería: Universidad de Almería.

Mavrogianopoulos, G., & Kyritis, S. (1989). The effect of day and night temperatures set points on yield of greenhouse tomatoes. *Agricoltura Mediterranea, 119*, 255–261.

Ooteghem, R. J. C. (2007). *Optimal control design for a solar greenhouse*. Wageningen: Wageningen University.

Peet, M. M., Willits, D. H., & Gardner, R. (1997). Response of ovule development and post-pollen production processes in male-sterile tomatoes to chronic, sub-acute high temperature stress. *Journal of Experimental Botany, 48*(306), 101–111.

Ross, J. (1975). Radiative transfer in plant communities. In J. L. Monteith (Ed.), *Vegetation and atmosphere* (pp. 13–55). London: Academic Press.

Sato, S., Peet, M. M., & Thomas, J. F. (2000). Physiological factors limit fruit set of tomato (Lycopersicon esculentum Mill.) under

chronic, mild heat stress. *Plant, Cell and Environment, 23*(7), 719–726.

Seginer, I., Gary, C., & Tchamitchian, M. (1994). Optimal temperature regimes for a greenhouse crop with a carbohydrate pool: a modelling study. *Scientia Horticulturae, 60*(1–2), 55–80.

Segura, M. L., Contreras, J. I., Salinas, R., & Lao, M. T. (2009). Influence of salinity and fertilization level on greenhouse tomato yield and quality. *Communications in Soil Science and Plant Analysis, 40*(1–6), 485–497.

Stanghellini, C. (1987). *Transpiration of greenhouse crops: An aid to climate management*. Wageningen: IMAG.

Stanghellini, C., & Bunce, J. A. (1993). Response of photosynthesis and conductance to light, CO_2, temperature and humidity in tomato plants grown at ambient and elevated CO_2. *Photosynthetica, 19*(4), 487–497.

Tap, F. (2000). *Economics-based optimal control of greenhouse tomato crop production*. Wageningen: Wageningen University.

Van Der Ploeg, A., & Heuvelink, E. (2005). Influence of sub-optimal temperature on tomato growth and yield: a review. *Journal of Horticultural Science and Biotechnology, 80*(6), 652–659.

Van Henten, E. J., Bakker, J. C., Marcelis, L. F. M., Van 't Ooster, A., Dekker, E., Stanghellini, C., et al. (2006). The adaptive greenhouse – An integrated systems approach to developing protected cultivation systems. *Acta Horticulturae, 718*, 399–406.

Van Straten, G., Vanthoor, B., Van Willigenburg, L. G., & Elings, A. (2006). A 'big leaf, big fruit, big substrate' model for experiments on receding horizon optimal control of nutrient supply to greenhouse tomato. *Acta Horticulturae, 718*, 147–155.

Vanthoor, B. H. E., Stanghellini, C., van Henten, E. J., & de Visser, P. H. B. (2011). A methodology for model-based greenhouse design: Part 1, a greenhouse climate model for a broad range of designs and climates. *Biosystems Engineering, 110*(4), 363–377.

Yakir, D., Rudich, J., & Bravdo, B. A. (1986). Adaptation to chilling: photosynthetic characteristics of the cultivated tomato and a high altitude wild species. *Plant, Cell and Environment, 9*(6), 477–484.

Zhang, J., Li, T., & Xu, J. (2008). Effects of sub-high temperature in daytime from different stages on tomato photosynthesis and yield in greenhouse. *Nongye Gongcheng Xuebao/Transactions of the Chinese Society of Agricultural Engineering, 24*(3), 193–197.